

Synthesis of $\text{Fe}_3\text{O}_4@ \text{SiO}_2@ \text{polymer}$ nanoparticles for controlled drug release

WU ChengLin, HE Huan, GAO HongJun, LIU Gan, MA RuJiang, AN YingLi & SHI LinQi*

Key Laboratory of Functional Polymer Materials, Ministry of Education; Institute of Polymer Chemistry, Nankai University, Tianjin 300071, China

Received November 23, 2009; accepted December 16, 2009

Novel multifunctional nanoparticles containing a magnetic $\text{Fe}_3\text{O}_4@ \text{SiO}_2$ sphere and a biocompatible block copolymer poly(ethylene glycol)-*b*-poly(aspartate) (PEG-*b*-PAsp) were prepared. The silica coated on the superparamagnetic core was able to achieve a magnetic dispersivity, as well as to protect Fe_3O_4 against oxidation and acid corrosion. The PAsp block was grafted to the surface of $\text{Fe}_3\text{O}_4@ \text{SiO}_2$ nanoparticles by amido bonds, and the PEG block formed the outermost shell. The anti-cancer agent doxorubicin (DOX) was loaded into the hybrid nanoparticles via an electrostatic interaction between DOX and PAsp. The release rate of DOX could be adjusted by the pH value.

magnetic nanoparticle, $\text{Fe}_3\text{O}_4@ \text{SiO}_2$, multifunctional, controlled drug release

1 Introduction

Magnetic nanoparticles have been widely used in such fields as catalysis, magnetic resonance image, and controlled drug release because of their special physical property [1–4]. Magnetic nanoparticles have been synthesized with a number of different compositions, such as Fe_3O_4 , spinel-type ferromagnets, and alloys. However, an unavoidable problem was that the magnetic nanoparticles were readily aggregated, oxidated, and eroded by acids, resulting in the loss of magnetism [5].

Surfactants or block copolymers were frequently employed to passivate the surface of the nanoparticles for increasing their stability and dispersity [6–10]. In general, surfactants or block copolymers were chemically anchored and physically adsorbed on the magnetic nanoparticles to form a single or double layer. For example, the modified Fe_3O_4 nanoparticles could be linked to the biocompatible block copolymers [11, 12]. However, the drawback of

polymer-coated magnetic nanoparticles was that they could not stabilize the active nanoparticles, and they were not stable in blood. Therefore, it is necessary to develop an effective method to protect magnetic nanoparticles. Biocompatible silica could be directly linked to the magnetic Fe_3O_4 nanoparticles, which formed a stable $\text{Fe}_3\text{O}_4@ \text{SiO}_2$ core-shell structure [13, 14]. The core-shell structure has such advantages as stability in low pH value, easy surface modification, and easy control of the shell thickness. However, the $\text{Fe}_3\text{O}_4@ \text{SiO}_2$ core-shell structure could not load drugs well. Thus, it is necessary to develop more complex structures for target-drug delivery systems.

Herein, the Stöber method and sol-gel processes were selected for coating magnetic nanoparticles with silica, and the biocompatible block copolymer of poly(ethyl glycol)-*b*-poly(aspartic acid) (PEG-*b*-PAsp) was subsequently linked to the surface of the silica to form multifunctional hybrid nanoparticles (Figure 1). The outer PEG could stabilize the nanoparticles as well as prevent the absorption, existing as long-circulating drug carriers. PAsp could be used to load the anticancer agent doxorubicin (DOX) due to the electrostatic interaction between the amino and carboxyl

*Corresponding author (email: shilinqi@nankai.edu.cn)



Figure 1 Synthesis of multilayer and multifunctional hybrid nanoparticles and the process of drug loading.

group, and the inner silica shell protects the magnetism of Fe_3O_4 . The hybrid nanoparticles with a multilayer and a multifunctional structure have potential applications in controlled drug release.

2 Experimental

2.1 Materials and experiment

Methoxy poly(ethylene glycol) ($\text{CH}_3\text{O}-\text{PEG}_{114}-\text{OH}$) ($M_w = 5000$, $\text{PDI} = 1.05$) was purchased from Across, USA. $\text{PEG}-\text{NH}_2$ was synthesized according to the previously reported procedure [15, 16]. Tetraethylorthosilicate (TEOS), (3-aminopropyl)triethoxysilane (APS), aspartic acid (Asp), 1-ethyl-3-(3-(dimethylamino)propyl) carbodiimide (EDC·HCl) were purchased from Alfa, USA. Doxorubicin hydrochlorate ($\text{DOX}\cdot\text{HCl}$) was purchased from Zhejiang Haizheng Co., China. Other chemicals are of analytical grade and used without further purification.

The number average molecular weight of the block copolymer $\text{PEG}-b-\text{PAsp}$ was calculated by $^1\text{H NMR}$. $^1\text{H NMR}$ spectra were obtained on a Varian UNITY-plus 400 M nuclear magnetic resonance spectrometer using CDCl_3 and D_2O as solvents. Dynamic light scattering (DLS) and static light scattering (SLS) measurements were performed on a laser light scattering spectrometer (BI-200SM) equipped with a digital correlator (BI-9000AT) at 636 nm. Transmission electron microscopy (TEM) measurements were conducted using a Philips T20ST electron microscope at an acceleration voltage of 200 kV. The drug loading capacity and release behavior were determined using a UV-vis 2550 spectrometer (Schimadu). The magnetic property was measured on a LDJ 9600 vibrating sample magnetometer at room temperature.

2.2 Synthesis of the $\text{PEG}-b-\text{PAsp}$ block copolymer

The block copolymer $\text{PEG}-b-\text{PAsp}$ was synthesized according to the previously reported procedure [15, 16], as illustrated in Figure 2. $\text{PEG}_{114}-\text{NH}_2$ (1.2 g, 0.24 mmol) was dissolved in CH_2Cl_2 (100 mL), and (γ -benzyl-L-glutamate *N*-carboxy-anhydride) (BLA-NCA) (6.0 g, 24.1 mmol) was added. The mixture was left to react for 72 h at 30 °C in nitrogen atmosphere. The product was precipitated into an

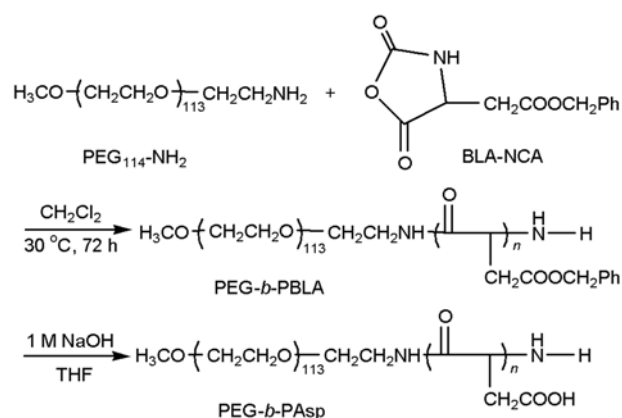


Figure 2 Synthesis of the $\text{PEG}-b-\text{PAsp}$ block copolymer.

excess of diethyl ether, and subsequently dried to a constant weight under vacuum (5.8 g, yield 80.6%).

$\text{PEG}-b-\text{PBLA}$ (5.8 g) was dissolved in THF (100 mL), and NaOH (150 mL, 1.0 mol/L) was added. The solution was retained at 25 °C for 10 h, and subsequently purified by dialysis to obtain the $\text{PEG}-b-\text{PAsp}$ block copolymer (2.46 g).

2.3 Synthesis of the well-dispersed Fe_3O_4 nanoparticles

The Fe_3O_4 nanoparticles were synthesized through co-precipitation with ferric and ferrous (2/1, mol/mol) according to the previously reported procedure [13]. $\text{FeCl}_3\cdot 6\text{H}_2\text{O}$ and $\text{FeCl}_2\cdot 4\text{H}_2\text{O}$ were dissolved in water (150 mL). The solution was subsequently heated to 80 °C after exhausting O_2 by N_2 . $\text{NH}_3\cdot\text{H}_2\text{O}$ (7 mL, 25%–28%) was added and reacted for another 6 h. The precipitate was isolated by an Nd-Fe-B magnet and washed with de-ionized water and ethanol. To obtain well-dispersed Fe_3O_4 nanoparticles, the precipitate was added to citric acid (0.2 M) and treated with ultrasonic.

2.4 Synthesis of the $\text{Fe}_3\text{O}_4@\text{SiO}_2$ nanoparticles

$\text{Fe}_3\text{O}_4@\text{SiO}_2$ nanoparticles were prepared by the previously reported Stöber method [17]. The magnetic nanoparticle Fe_3O_4 (30 mg) was dissolved in mixed solution of water (30 mL) and ethanol (150 mL). Ammonia solution (3.5 mL) and TEOS (500 μL , 460 mg) were added to the mixed solution with stirring and reacted for 5 h. After that, APS (250 μL) was added. The nanoparticles were isolated by an Nd-Fe-B magnet and washed with ethanol.

2.5 Synthesis of the hybrid nanoparticles and drug loading

$\text{Fe}_3\text{O}_4@\text{SiO}_2-\text{NH}_2$ (50 mg) was dissolved into water (10 mL), and $\text{PEG}-b-\text{PAsp}$ (10 mL, 50.0 g/L) was added to the solution with stirring for 10 min (300 r/s). After that, the mixed solution (10 mL) of EDC·HCl (42.3 mg) and NHS (7.9 mg) was added and reacted for 4 h at 0 °C. The drug of

DOX·HCl (32.5 mg) was added with stirring. After dialysis for removing the unloaded DOX, the DOX-loaded hybrid nanoparticles were prepared.

2.6 DOX release from the hybrid nanoparticles

A given amount of the DOX-loaded hybrid nanoparticles was dissolved into water with a concentration of 1.0 g/L. The release process of DOX from the hybrid nanoparticles was studied at different pH values (pH 4.9, 5.8, and 7.4) using a UV-vis 2550 spectrophotometer. 4 mL of the solution was transferred into a dialysis bag, which was subsequently placed into 16 mL buffer solution. Aliquots of 4 mL were periodically withdrawn from the buffer solution to containers. The volume of the solution was retained constant by adding 4 mL of buffer solution after each sampling. The DOX content and DOX-loaded efficiency were measured by UV-Vis spectrophotometer at 485 nm.

3 Results and discussion

3.1 Synthesis of the PEG-*b*-PAsp block copolymer

The diblock copolymer PEG-*b*-PAsp was synthesized through ring opening polymerization (ROP) with PEG-NH₂ as an initiator. Figure 3 showed the ¹H NMR spectra of PEG-*b*-PBLA and PEG-*b*-PAsp. The resonance bands observed in the regions of 3.6 (a) ppm and 5.16 (d) ppm were attributed to methylene protons of PEG and pendent methylene protons of PBLA. Based on the relative intensities, the number-average molecular weight of PEG-*b*-PBLA was calculated. The block copolymer was denoted as PEG₁₁₄-*b*-PBLA₉₀, with the subscript indicating the number of repeating units. Compared to the ¹H NMR spectra of PEG-*b*-

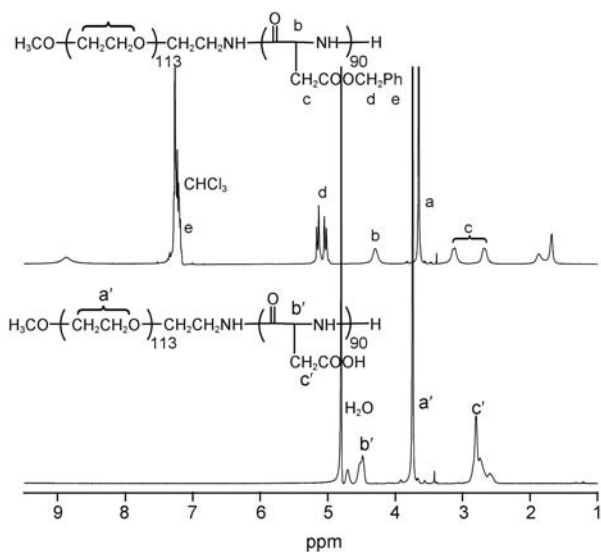


Figure 3 ¹H NMR spectra of PEG-*b*-PBLA and PEG-*b*-PAsp diblock copolymers.

PBLA and PEG-*b*-PAsp, the resonance bands observed in the regions of 5.16 (d) and 7.27 (e) disappeared, indicating PBLA was fully hydrolyzed to PAsp.

3.2 Synthesis of magnetic nanoparticles

Magnetic nanoparticles were prepared using the co-precipitation method, which was a facile and convenient way to synthesize Fe₃O₄ nanoparticles. The size, shape, and composition of the magnetic nanoparticles depended on the Fe²⁺/Fe³⁺ ratio, reaction temperature, and pH value [5]. Such long-chain surfactants as oleic acid and lauric acid were frequently used to stabilize the magnetic nanoparticles [18]. Figure 4(a) shows the TEM image of Fe₃O₄ nanoparticles modified by citric acid. The diameter of the nanoparticles was 6–8 nm with a narrow size distribution.

Fe₃O₄@SiO₂ was synthesized using the Stöber method and sol-gel process. The thickness of SiO₂ was readily varied by changing the amount of TEOS, the concentration of ammonia, and the ratio of TEOS to water. The advantage of this method was that there were numerous hydroxyl groups on the surface of silica, which were readily linked to other groups. Figure 4(b) shows the TEM image of Fe₃O₄@SiO₂ nanoparticles. The diameter of Fe₃O₄@SiO₂ nanoparticles

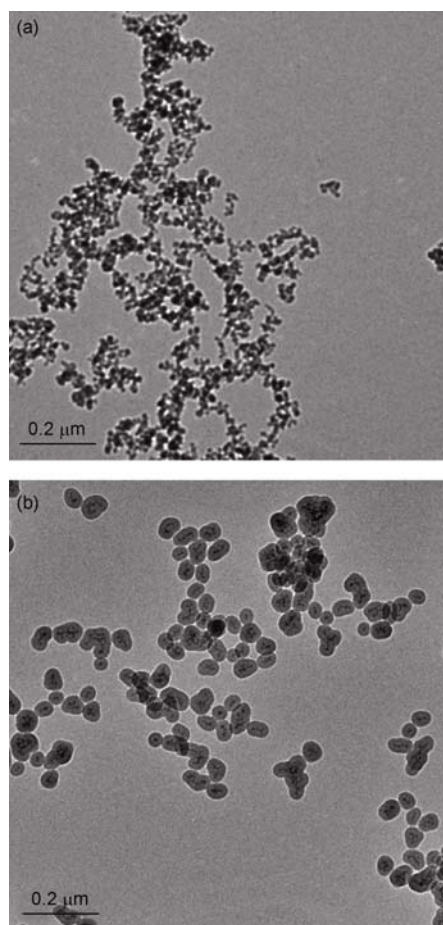


Figure 4 TEM images of Fe₃O₄ (a) and Fe₃O₄@SiO₂ (b) nanoparticles.

was about 60 nm with a narrow size distribution.

3.3 The diameter of the DOX-loaded hybrid nanoparticles

The anticancer agent DOX could be loaded to the hybrid nanoparticles via the electrostatic interaction. Figure 5 shows the hydrodynamic diameter distribution ($f(D_h)$) of the DOX-loaded hybrid nanoparticles measured by DLS at the scattering of 90 °C. The DOX-loaded hybrid nanoparticles had a narrow distribution, and the average hydrodynamic diameter D_h was about 128 nm.

Figure 6 shows the angular dependence of the translational diffusion coefficient D_t of the DOX-loaded hybrid nanoparticles at the concentration of 0.2 g/L. The value of the translated diffusion coefficient D_t^0 could be calculated by extrapolating q^2 ($q = 4\pi\sin(\theta/2)/\lambda_0$) to 0, and the hydrodynamic radii R_h^0 could be calculated by the Stokes-Einstein equation ($D_h = K_B T / 3\pi\eta D_t$). The D_h^0 of the DOX-loaded hybrid nanoparticles was 172.6 nm.

The values of R_g , R_h^0 , and R_g/R_h^0 of the DOX-loaded hybrid nanoparticles were 62.8 nm, 86.3 nm and 0.727, respectively. The R_g/R_h^0 value revealed the morphology of nanopar-

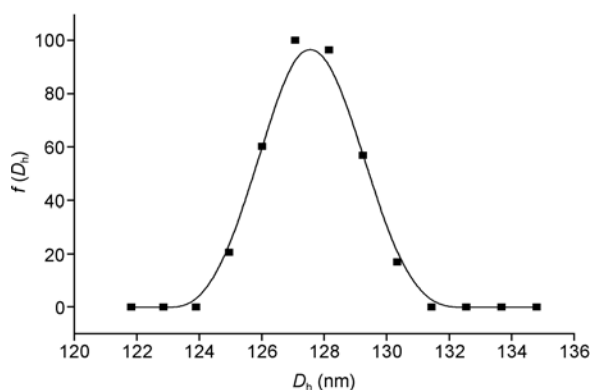


Figure 5 Hydrodynamic diameter distribution ($f(D_h)$) of the DOX-loaded hybrid nanoparticles.

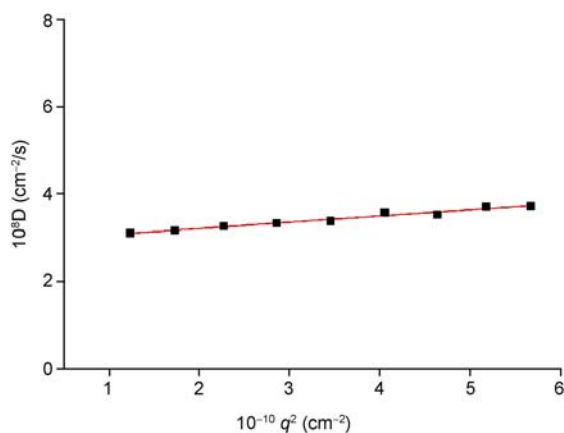


Figure 6 Angular dependence of the translational diffusion coefficient of the DOX-loaded hybrid nanoparticles.

ticles in aqueous solution. For a uniform sphere, $R_g/R_h^0 \sim 0.775$, a hollow structure, $R_g/R_h^0 \sim 1.0$, a random coil chain in good solvent, $R_g/R_h^0 \sim 1.5$, and a rigid chain in solvent, $R_g/R_h^0 \sim 2.0$ [19]. Herein, R_g/R_h^0 of the hybrid nanoparticles was 0.727, indicating the hybrid nanoparticles had a uniform sphere structure.

3.4 Drug release

DOX is a widely used anticancer agent for the treatment of such forms of cancer as leucocythemia and breast cancer. The use of it is limited in practice, because it is readily absorbed in the blood after injection and is harmful to normal tissues. Thus it is meaningful to develop targeting carriers of DOX.

The drug loading efficiency was 4.0% (DOX loading efficiency (%) = $100W_{DOX}/(W_{DOX} + W_{nano})$). The pH-responsive release profiles from the hybrid nanoparticles are shown in Figure 7 (pH 4.9, 5.8, and 7.4). The release rate decreased with the increase of pH values. The pK_a value of the amino group in DOX is about 8.2 [20]. Thus the electrostatic interaction existed at neutral surrounding and disappeared at acid surrounding. The pH value of the tumor was 5.0–6.0, which was lower than the pH value of the normal tissue, so the DOX on hybrid nanoparticles could be released at the tumor.

3.5 Magnetism test

The superparamagnetic property and the high saturation magnetization value are two significant parameters for controlled drug release. Superparamagnetism is the responsiveness to an applied magnetic field without retaining any magnetism after removal of the applied magnetic field [21]. Figure 8 shows the magnetization curves of Fe_3O_4 (a), $Fe_3O_4@SiO_2$ (b), and the hybrid nanoparticles (c) at room temperature. As shown in Figure 8, the saturation magnetization values (M_s) of the Fe_3O_4 , $Fe_3O_4@SiO_2$ and the hybrid nanoparticles were respectively 35.1, 7.49, and 2.35 emu/g.

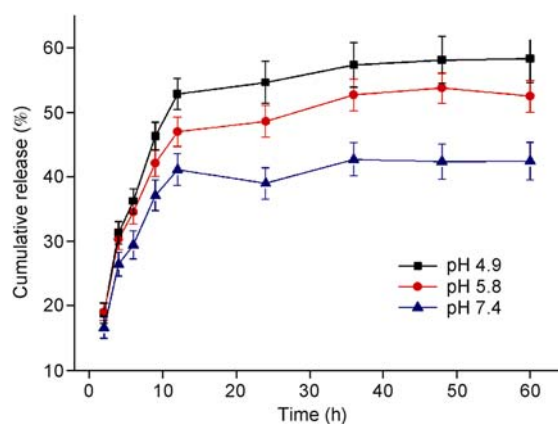


Figure 7 Release profiles of DOX from the hybrid nanoparticles at different pH values (pH 4.9, 5.8, and 7.4).

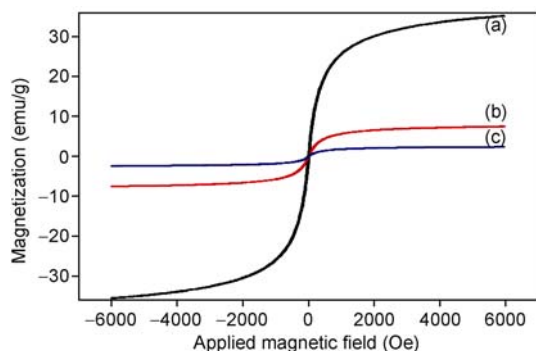


Figure 8 Magnetization curves of Fe_3O_4 (a), $\text{Fe}_3\text{O}_4@SiO_2$ (b), and the hybrid nanoparticles (c) at room temperature.

Three magnetization curves followed a Langevin behavior over the applied magnetic field and the coercivity (H_c) of the hybrid nanoparticles (lower than 20 Oe) could be ignored, which was regarded as superparamagnetism. Thus the hybrid nanoparticles have potential applications in targeting drug delivery systems.

4 Conclusions

Well-dispersed magnetic Fe_3O_4 (6–8 nm) nanoparticles were prepared using the co-precipitation method. Core-shell $\text{Fe}_3\text{O}_4@SiO_2$ nanoparticles were synthesized using the Stöber method and sol-gel process. The biocompatible block copolymer PEG-*b*-PASP was grafted to the surface of the biocompatible $\text{Fe}_3\text{O}_4@SiO_2$ nanoparticles via the amide bond. Thus the hybrid nanoparticles with multifunctions and multilayers were prepared. The anticancer agent DOX was loaded to the hybrid nanoparticles via the electrostatic interaction, and was identified to release faster at low value (pH 4.9) than the normal pH of human bodies (pH 7.4). The hybrid nanoparticles have potential applications in the treatment of cancer as targeting drug-delivery carriers.

This work was supported by the National Natural Science Foundation of China (Grant Nos. 20774051, 50625310, and 50830103), and the Opening Foundation of Sichuan University.

- Perez JM, O'Loughin T, Simeone FJ, Weissleder R, Josephson L. DNA-based magnetic nanoparticle assembly acts as a magnetic relaxation nanoswitch allowing screening of DNA-cleaving agents. *J Am Chem Soc*, 2002, 124: 2856–2857
- Kinsella JM, Ivanisevic A. Enzymatic clipping of DNA wires coated with magnetic nanoparticles. *J Am Chem Soc*, 2005, 127: 3276–3277
- Xu CJ, Xu KM, Gu HW, Zheng RK, Liu H, Zhang XX, Guo ZH,

- Xu B. Dopamine as a robust anchor to immobilize functional molecules on the iron oxide shell of magnetic nanoparticles. *J Am Chem Soc*, 2004, 126: 9938–9939
- Kim J, Lee JE, Lee J, Yu JH, Kim BC, An K, Hwang Y, Shin C, Park J, Kim J, Hyeon T. Magnetic fluorescent delivery vehicle using uniform mesoporous silica spheres embedded with monodisperse magnetic and semiconductor nanocrystals. *J Am Chem Soc*, 2006, 128: 688–689
- Lu AH, Salabas EL, Schüth F. Magnetic nanoparticles: synthesis, protection, functionalization, and application. *Angew Chem Int Ed*, 2007, 46: 1222–1244
- Yang XQ, Chen YH, Yuan RX, Chen GH, Blanco E, Gao JM, Shuai XT. Folate-encoded and Fe_3O_4 -loaded polymeric micelles for dual targeting of cancer cells. *Polymer*, 2008, 48: 3477–3485
- Chang Y, Bai YP, Teng B, Li ZL. A new drug carrier: Magnetite nanoparticles coated with amphiphilic block copolymer. *Chin Sci Bull*, 2009, 54: 1190–1196
- Hu F X, Neoh KG, Kang ET. Synthesis of Folic acid functionalized PLLA-*b*-PPEGMA nanoparticles for cancer cell targeting. *Macromol Rapid Commun*, 2009, 30: 609–614
- Ren J, Jia MH, Ren TB, Yuan WZ, Tan QG. Preparation and characterization of PNIPAAm-*b*-PLA/ Fe_3O_4 thermo-responsive and magnetic composite micelles. *Mater Lett*, 2008, 62: 4425–4427
- Guo M, Yan Y, Zhang HK, Yan HS, Cao YJ, Liu KL, Wan SR, Huang JS, Yue W. Magnetic and pH-responsive nanocarriers with multilayer core-shell architecture for anticancer drug delivery. *J Mater Chem*, 2008, 18: 5104–5112
- Lu J, Ma S, Sun JY, Xia CC, Liu C, Wang ZY, Zhao X, Gao FB, Gong QY, Song B, Shuai XT, Ai H, Gu ZW. Manganese ferrite nanoparticle micellar nanocomposites as MRI contrast agent for liver imaging. *Biomaterials*, 2009, 30: 2919–2928
- Thümenmann AF, Schütt D, Kaufner L, Pison U, Möhwald H. Maghemite nanoparticles protectively coated with poly(ethylene imine) and poly(ethylene oxide)-*block*-poly(glutamic acid). *Langmuir*, 2006, 22: 2351–2357
- Chen FH, Gao Q, Ni JZ. The grafting and release behavior of doxorubicin from $\text{Fe}_3\text{O}_4@SiO_2$ core-shell structure nanoparticles via an acid cleaving amide bond: the potential for magnetic targeting drug delivery. *Nanotechnology*, 2008, 19: 165103
- Santra S, Tapeç R, Theodoropoulou N, Dobson J, Hebard A, Tan WH. Synthesis and characterization of silica-coated iron oxide nanoparticles in microemulsion: the effect of nonionic surfactants. *Langmuir*, 2001, 17: 2900–2906
- Wang XJ, Sun JP, Li AD. Synthesis of PEG- NH_2 . *Fine Chem Inter*, 2006, 36: 40–42
- Ma JB, Zhang GL, Wu QH. Synthesis and characterization of diblock copolymer PEG-*b*-PBLA. *Acta Polym*, 2004, 2: 223–227
- Lu Y, Yin YD, Mayers BT, Xia YN. Modifying the surface properties of superparamagnetic iron oxide nanoparticles through a sol-gel approach. *Nano Lett*, 2002, 2: 183–186
- Wormuth K. Superparamagnetic latex via inverse emulsion polymerization. *J Colloid Interf Sci*, 2001, 241: 366–377
- Tu YF, Wang XH, Zhang D, Zhou QF, Wu C. Self-assembled nanostructure of a novel coil-rod diblock copolymer in dilute solution. *J Am Chem Soc*, 2000, 122: 10201–10205
- Sturgeon RJ, Schulman SG. Electronic absorption spectra and protolytic equilibria of doxorubicin: direct spectrophotometric determination of microconstants. *J Pharm Sci*, 1977, 66: 958–961
- Fu FX, Neoh KG, Kang ET. Synthesis and in vitro anti-cancer evaluation of tamoxifen-loaded magnetite/PLLA composite nanoparticles. *Biomaterials*, 2006, 27: 5725–5733